

Vehicle Dynamics, Lateral Forces, Roll Angle, Tire Wear and Road Profile States Estimation - A Review

Riton Kumer Das, Md. Abu Mowazzem Hossain^(*), Md. Tazul Islam, Sajal Chandra Banik

Department of Mechanical Engineering, Chittagong University of Engineering & Technology, Chattogram 4349, BANGLADESH
e-mail: rkdas2608@gmail.com

^(*) Corresponding Author: mowazzem@cuet.ac.bd

SUMMARY

Estimation of vehicle dynamics, tire wear, and road profile are indispensable prefaces in the development of automobile manufacturing due to the growing demands for vehicle safety, stability, and intelligent control, economic and environmental protection. Thus, vehicle state estimation approaches have captured the great interest of researchers because of the intricacy of vehicle dynamics and stability control systems. Over the last few decades, great enhancement has been accomplished in the theory and experiments for the development of these estimation states. This article provides a comprehensive review of recent advances in vehicle dynamics, tire wear, and road profile estimations. Most relevant and significant models have been reviewed in relation to the vehicle dynamics, roll angle, tire wear, and road profile states. Finally, some suggestions have been pointed out for enhancing the performance of the vehicle dynamics models.

KEYWORDS: vehicle dynamic; tire friction; tire wear; road profile; roll angle.

1. INTRODUCTION

In the automotive industry, vehicle safety and quality assurance are important factors to ensure manufacturing and maintenance performance. For the successful functioning of an advanced chassis control system, proper information about the vehicle dynamic states is essential to know as shown in Figure 1. For example, the electronic stability control module can optimize the active longitudinal and lateral tire forces online. Through effective design and implementation of advanced chassis control systems can greatly reduce the risk of accidents [1]. As a result, the problem of estimating the state of the vehicle has received considerable attention from many researchers.

There are also vehicle dynamics and adjustments of the wheel characteristic angles needed for this purpose [2]. Wheel camber angles affect the steering stability and controllability of the vehicle; hence, the alignment of the wheels and the vehicle control system poses a significant

problem. In addition, the toe angles are related to driving comfort, fuel efficiency, and tire life [3]. It should be noted that misalignment of wheels results in an accident and rapid tire wear, which is not expected. Moreover, it decreases the controllability of the vehicle.

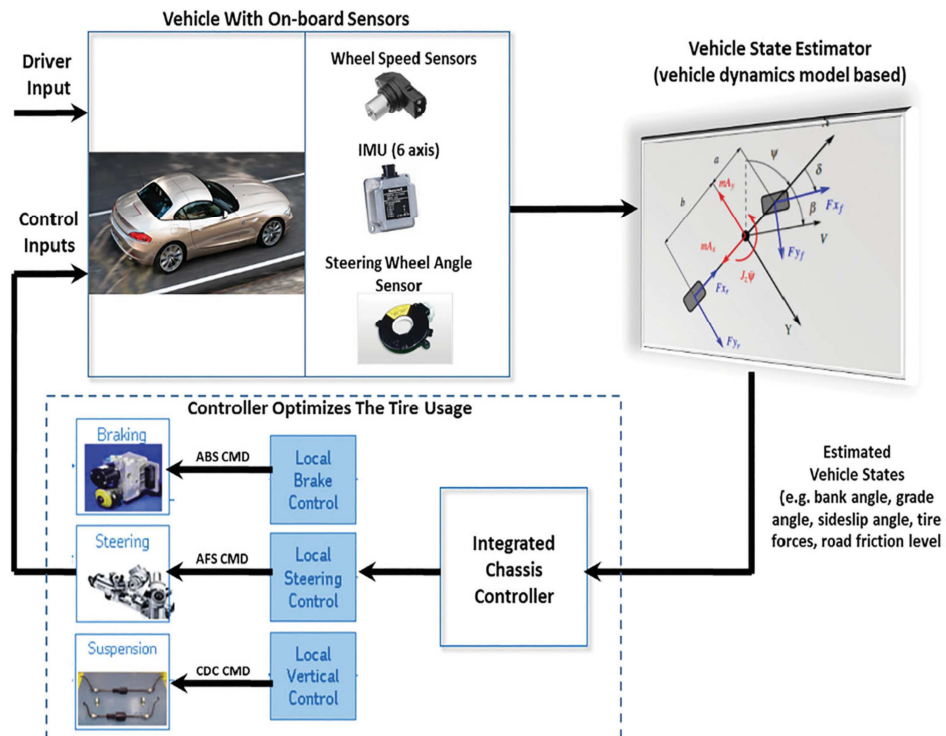


Fig. 1 Representation of an integrated chassis control system [1]

2. CRUCIAL PARAMETERS

The lateral forces of the vehicle, the sideslip angle, the roll angle, the tire friction, and tire wear need to be analysed for accurate actuation of vehicle system dynamics. For proper performance of vehicle dynamic stability, it is necessary to know the vehicle state information, proper knowledge of longitudinal and lateral forces of the tire, sideslip angle, and road profile at the right time. These attributes are critical to measuring with adequate precision due to high costs and other associated inconveniences. The vehicle dynamic state's knowledge can significantly reduce vehicle accident and fuel consumption as well as increases social positive impact through the feasible model and the implantation of advanced vehicle dynamic control methods. In this respect, a number of studies have been carried out to estimate the problem of the dynamic state of the vehicle.

This article presents a state-of-the-art review on vehicle state estimation approaches utilized in vehicle stability and control applications. This review article focused on tire lateral forces and estimation models used in vehicle dynamic stability. A summary of important methodologies on the vehicle road profile estimation, tire wear estimation approaches, roll profile estimation approaches, and roll angle estimation approaches are presented.

3. CRUCIAL VARIABLES

Vehicle dynamics play an important role to develop the modern vehicle industry because of the increasing demand for vehicle safety, intelligent control, and environmental protection. Researchers have studied the vehicle dynamics in a set of DoF (Degree of Freedom) of vehicle reference using some important variables [4-6]: i) Lateral dynamics: it controls the vehicle stability and handling; its variables are sideslip angle (β), lateral displacement (y), and yaw angle (turn around the z-axis, ψ), ii) Longitudinal dynamics: it determines the vehicle stability performance and the variables are rotational velocity (ω), longitudinal velocity (Vx) and tire slip ratio (λ), and iii) Vertical dynamics: it makes comfort for the passengers and the variables are vibration reduction roll (turn around the x-axis, θ), pitch (turn around the y-axis, ϕ), and vertical acceleration [7,8], and these important variables are depicted in Figure 2. In the first step, the overall characteristics of vehicle dynamics can be visualized using simple mechanical models such as planer two-wheel models, third planer models, 3D models, etc. [9]. In these fundamental models, basic behaviours can be characterized with respect to the longitudinal, lateral, vertical motion, pitch, and roll using various linear models [10]. The vehicle models are developed for the component parts and characterized by sub-models of the vehicle. However, the use of vehicle dynamic models depends on the degree of ingoing relation to the handling quality. In addition, overall characteristics can be interpreted by utilizing the process of multi-body system (MBS) simulations or programming [11]. A summary of the vehicle state estimation and models is presented in Table 1.

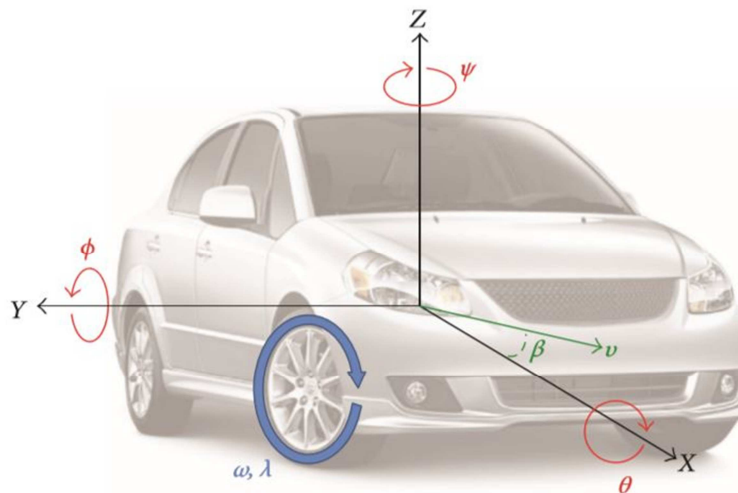


Fig. 2 Vehicle dynamic variables and reference methods [7]

Table 1 A summary of the different models used for estimating vehicle states

Model used	Methodology	Estimated states	Reference
Four-wheel vehicle model	Extended Kalman Filter and Unscented Kalman Filter	Indicator, vehicle and tire-road friction coefficient	[12]
Single-track model	Extended Kalman Filter and Sliding Model Observer	Tire forces and sideslip angle	[13]
Kinematics model	Nonlinear observer	Vehicle sideslip angle	[14]
Longitudinal dynamics	Recursive Least Square	Vehicle mass	[15]
Vehicle planar model, Vehicle wheel dynamics model and	Model based analysis	Vehicle parameter estimation and tire forces	[16]

<i>Wheel friction ellipse</i>			
<i>Four-wheel vehicle model</i>	<i>Unscented Kalman Filter process</i>	<i>Lateral tire -road forces, tire-road friction coefficient and wheel sideslip angle</i>	<i>[17]</i>
<i>Yaw plane model</i>	<i>Recursive Least Square</i>	<i>Vehicle sideslip angle</i>	<i>[18]</i>
<i>Fuzzy logic</i>	<i>Intelligent Tire Prototype/Computational method</i>	<i>Slip angle and vertical load estimation</i>	<i>[19]</i>
<i>Accelerometer Based</i>	<i>Tire mounted sensors</i>	<i>Tire load and slip angle</i>	<i>[20]</i>
<i>Vehicle dynamic model</i>	<i>Point mass</i>	<i>Vehicle parameters</i>	<i>[21]</i>
<i>Kinematic model</i>	<i>Time varying gains</i>	<i>Grade angles and road bank</i>	<i>[22]</i>
<i>Gaussian white noise and one-order low pass filter</i>	<i>Kalman Filter Algorithm</i>	<i>Roll angle</i>	<i>[23]</i>
<i>Roll motion model and bicycle model</i>	<i>Finite Impulse Response (FIR)</i>	<i>Roll angle and bank angle</i>	<i>[24]</i>
<i>Sensor Fusion method</i>	<i>Integrated Neural Network and Kalman Filter</i>	<i>Roll angle</i>	<i>[25]</i>
<i>Kinematics model based</i>	<i>Rule Based</i>	<i>Vehicle longitudinal velocity</i>	<i>[26]</i>
<i>High Mobility Multipurpose Wheeled Vehicle (HMMWV)</i>	<i>Electro-mechanical Continuously Variable Transmission (CVT)</i>	<i>Vehicle longitudinal dynamic</i>	<i>[27]</i>
<i>Two track vehicle dynamic model</i>	<i>Two Extended Kalman Filter</i>	<i>Sideslip angle, tire wear</i>	<i>[28]</i>
<i>Nonlinear lateral 3DoF dynamic model</i>	<i>Hydro-pneumatic</i>	<i>Tire wear</i>	<i>[28]</i>
<i>Nonlinear vehicle model</i>	<i>Extended Kalman Filter</i>	<i>Tire forces</i>	<i>[29]</i>
<i>Four-wheel vehicle model</i>	<i>Luenberger observer, Extended Kalman Filter</i>	<i>Tire forces and road grade</i>	<i>[30,31]</i>

3.1 USEFUL EQUATIONS

Vehicle dynamics modelling as a function of tire-road forces is very complex as many environmental features and tire characteristics (applied load, tire pressure, road surface) are involved. In the past, many researchers have used a variety of models to model these forces. Some of the important formulas are presented in this section.

Ghandour et al. [12] estimated the maximum lateral friction coefficient using the Dugoff tire model and the iterative nonlinear optimization method of Levenberg-Marquardt. They have used the Dugoff tire model because it accurately measures the lateral forces with a few parameters [12,17]. The mathematical formula for the Dugoff tire model as:

$$F_{yij} = -C_{\alpha i} \tan \alpha_{ij} f(\lambda) \quad (1)$$

where F_{yij} (N) is the lateral force on the (ij) tire, $C_{\alpha i}$ (N/rad) is the cornering stiffness and $f(\lambda)$ is given by the following equation:

$$f(\lambda) = \begin{cases} (2 - \lambda)\lambda, & \text{if } \lambda < 1 \\ 1, & \text{if } \lambda \geq 1 \end{cases} \quad (2)$$

The longitudinal and lateral velocities at the CG are governed by the equations of motion as [14]:

$$\dot{v}_x = a_x + \dot{\psi}v_y, \quad (3)$$

$$\dot{v}_y = a_y + \dot{\psi}v_x, \quad (4)$$

where, v_x and v_y are the longitudinal and lateral velocities, a_x and a_y are the longitudinal and lateral accelerations, and $\dot{\psi}$ is the yaw rate.

Fathy et al. [15] proposed a simple longitudinal vehicle dynamics model by considering drag, road grade-induced, and rolling resistance forces as:

$$m\dot{v}_x = F_e - F_b - \frac{1}{2}\rho A_d C_d V_x^2 - mg \sin \zeta - mg f_r \cos \zeta \quad (5)$$

Here, m denotes the mass of the vehicle and v_x denotes its longitudinal velocity. F_e is the effective engine force at the wheels and F_b is the effective braking force at the wheels.

$\frac{1}{2}\rho A_d C_d V_x^2 =$ Aerodynamic drag; where, ρ is the air density, A_d is the effective frontal area, C_d is a drag coefficient and V is the longitudinal vehicle velocity.

$mg f_r \cos \zeta =$ Rolling resistance; where f_r is constant fraction and ζ is road grade angle

$mg \sin \zeta =$ Resistance force due to the road grade

The tire slip ratio is defined as follows [16]:

$$\sigma = \frac{R_e \omega - v_w \cos \beta}{\max\{R_e \omega, v_w \cos \beta\}} \quad (6)$$

Where, R_e is the effective tire radius and ω is the angular velocity of the tire. β , is called the tire slip angle and the direction of the tire velocity, v_w .

If the pitch dynamic effects on roll motion are neglected, the roll angle can be calculated as [25]:

$$\theta = \frac{\Delta_{11} - \Delta_{12} + \Delta_{21} - \Delta_{22}}{2e_f} - \frac{m_v a_{ym} h}{k_t} \quad (7)$$

where Δ_{ij} is the suspension deflection, a_{ym} is the lateral acceleration, k_t is the roll stiffness resulting from tire stiffness and m_v is the vehicle weight.

The measured lateral acceleration a_{ym} is given by [22]:

$$a_{ym} = a_y + g \cos \vartheta \sin \varphi \quad (8)$$

Here, ϑ is the pitch angle and φ is the roll angle.

And lateral acceleration a_y from rigid body kinematics can be written as [22]:

$$a_y = \dot{v}_y + \omega_z v_x - \omega_x v_z \quad (9)$$

Where, $\underline{v} = (v_x, v_y, v_z)$ is the velocity vector of the center of gravity (CoG) and $\underline{\omega} = (\omega_x, \omega_y, \omega_z)$ is the vector of tum rates (roll, pitch, and yaw-rate).

The longitudinal and lateral translational motion and the yaw rotational movement can be found from the vehicle's dynamic motion model [31]:

$$\begin{cases} \dot{v}_x = \frac{1}{m} \sum F_{xi} + \dot{\psi} v_y \\ \dot{v}_y = \frac{1}{m} \sum F_{yi} - \dot{\psi} v_x \\ \ddot{\psi} = \frac{1}{I_z} \sum M_{zi} \end{cases} \quad (10)$$

Here, I_z the moment of inertia. F_{xi} , F_{yi} and M_{zi} are respectively the longitudinal and lateral tire/road forces and the rotational moment around the vertical axis ($i = 1; 2; 3; 4$ represents the four wheels of the vehicle).

3.2 TIRE LATERAL FORCES

Tire lateral force functions are related to the camber angle and sideslip angle and it is proportional to both of them, as shown in Figure 3. The camber angle provides vehicle stability by adjusting or increasing the lateral forces for keeping on the road. Therefore, the camber angles can be adjusted for controlling the lateral force when out of control of the sideslip angle [32]. For controlling the caster angle, lateral force or camber angle can also be used. The steering axis leaning of the wheel can be demonstrated by two-sided angles: lean angle and caster angle. The behaviour of the camber and sideslip angles are depicted in Figures 4 and 5. The sideslip angle is the main cause of the lateral force. Thus, the camber thrust or lateral force is generated by changing the camber angle and it is comparatively lower than the lateral force produced by the sideslip angles [33]. The lateral force generated by the sideslip angle is ten times more than the lateral force by indicating the camber angle, as seen in Figures 4 and 5.

Numerous studies focused on lateral force as in [34-36]. Cho et al. [37] presented a comprehensive example which shows a depiction of simultaneous longitudinal force and lateral force estimation using a random-walk Kalman filter technique. From the simulation, the researchers found how the tire force estimator performs under different driving conditions that there are adequate steering wheel functions. Researchers in [38-42] devoted the lateral tire forces and investigated two observations based on Unscented [43] and the Extended Kalman filter [44,45] methods. This Extended Kalman filter is a nonlinear model of the Kalman filter method. Jacobian matrices [46] linearize the nonlinear filter with the current mean and covariance. However, the Extended Kalman Filter is simple as it agonizes from instability because of erroneous parameters and linearization. In addition, the Jacobian matrix calculation is costly. For this inconvenience, the Unscented Kalman filter is useful as it utilizes a deterministic sample technique with a minimal set of a sample points to capture the covariance and mean [47]. Pattathil et al. [33] developed a 1D-tire model to synthesis under the optimal 1D slop functions of a tire force, which is an important factor for the vehicle controlling of a metric estimation such as steering impressibility, roll gradient and understeer. They utilize a magic formula known as Pacejka's tire model for the lateral force model and sideslip angle.

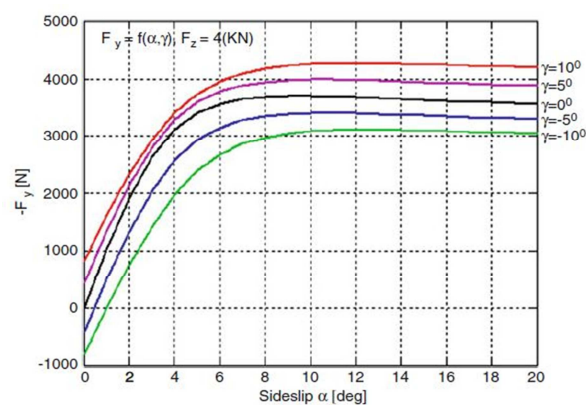


Fig. 3 Tire lateral force of the camber angle and the sideslip angle [48]

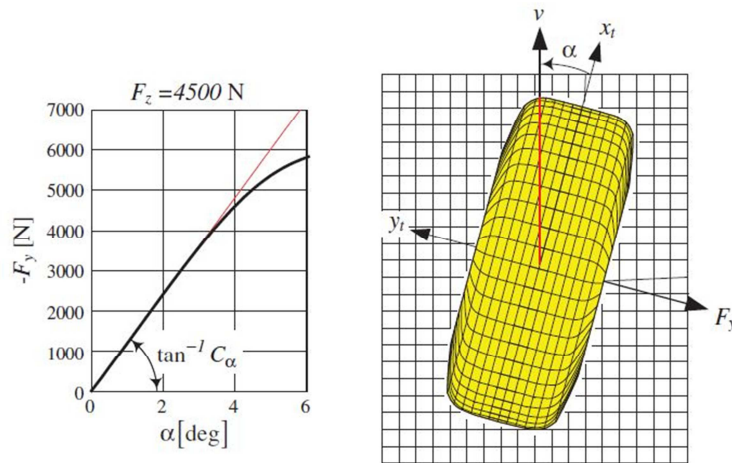


Fig. 4 Generated the tire sideslip force (F) and the sideslip angle (α) at the top view [32]

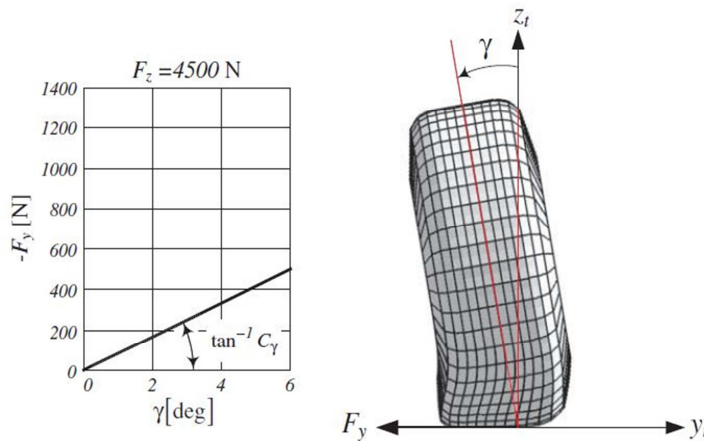


Fig. 5 Generated the tire camber force (F) and the camber angle (γ) at the front view [32]

3.3 TIRE WEAR ESTIMATION

The tire wear problem tends to be a significant issue due to its greater impact on vehicle and driving safety. Uneven tire wear is a serious problem when the wheel alignment parameters are not in the proper range or acceptable range. In addition to that, the tire issue will not only affect an economic point but also impacts environmental pollution [49]. Researchers studied this tire wear issue for two aspects: macroscopic wear vehicle dynamics and microscopic wear mechanism [28].

From the microscopic point of view, [50] carried out a theoretical study from the rubber wear mechanism aspect on tire wear issue. Researchers in [51,52] utilized the finite element method (FEM) for tire wear estimation. While Tembleque et al. [53] conducted the issue of tire wear and tire rolling resistance using the boundary element method (BEM).

From the vehicle dynamic macroscopic point of view, two techniques that can be utilized to study tire wear problems are experimental and simulated. Knisley [54] utilized the experimental approach for the outdoor driving environment and provided related theory-based tire wear data. In the simulation approach, Ma et al. [55] discussed the decrement of tire

wear from two views: the torque distribution and optimization of the Ackerman steering angle. Shen et al. [56] designed a hierarchical controller to measure the necessary yaw torque and driving force of wheels and how it decreased the tire wear rate.

3.4 TIRE FRICTION ESTIMATION

Besides the tire and dynamic states of the vehicle, it is expected that instant knowledge of tire-road friction potential including anti-lock braking systems (ABS), adaptive cruise control, electronic stability control (ESC), and collision avoidance systems can improve the performance of many active chassis control. Many researchers have revealed the estimate of tire-road friction, which is one of the most important issues for the tire condition and vehicle manufacturers, which can decrease vehicle crashes [57]. Schinkel et al. [58] have discussed that tire friction force affects vehicle stability and performance. The researchers estimated road and tire friction using the algorithm for two approaches, such as experimental and model-based. In the experimental approach, it is endeavoured to find a correlation between road and tire friction-related parameters and sensor data (temperature sensor, acoustic sensor, etc.). While the model-based ways to estimate the friction condition using mathematical models and it is divided into three main categories: sideslip-based approach, vehicle dynamic type approach, and tire model-based type approach. A review article has discussed these approaches briefly in [57]. Researchers assumed that the sideslip ratio and tire friction conditions have a linear relation at a low sideslip ratio [59,60]. Kalman filter, Extended Kalman Filter (EKF), and Global Positioning System (GPS) approaches are also used to find correlations between friction coefficient and vehicle parameters. Using GPS, coordinates can be displayed accurately. Consequent to the road and tire friction features, tires have utmost braking force when the normalized brake stiffness becomes zero. The least-square algorithm and the Euler approximation theory are utilized to calculate the braking stiffness at zero position. However, these techniques are appropriate for theoretical study and difficult to utilize due to higher cost, timeliness, and low accuracy of recognition [59]. Li et al. [61] suggested an extensive technique for road and tire friction estimation expressed on the signal fusion method under the complex method including driving, steering, and braking and this technique is more accurate and relatively easy to satisfy the control demands. In [39], the authors proposed a combined Auxiliary Particle Filter (APF) and Iteration Extended Kalman Filter (IEKF) method. They determined the vehicle tire-road friction coefficient through an iteration algorithm and proved that this method was also more accurate and real-time estimation. They compared their results at high friction coefficient and low friction coefficient, as shown in Figure 6.

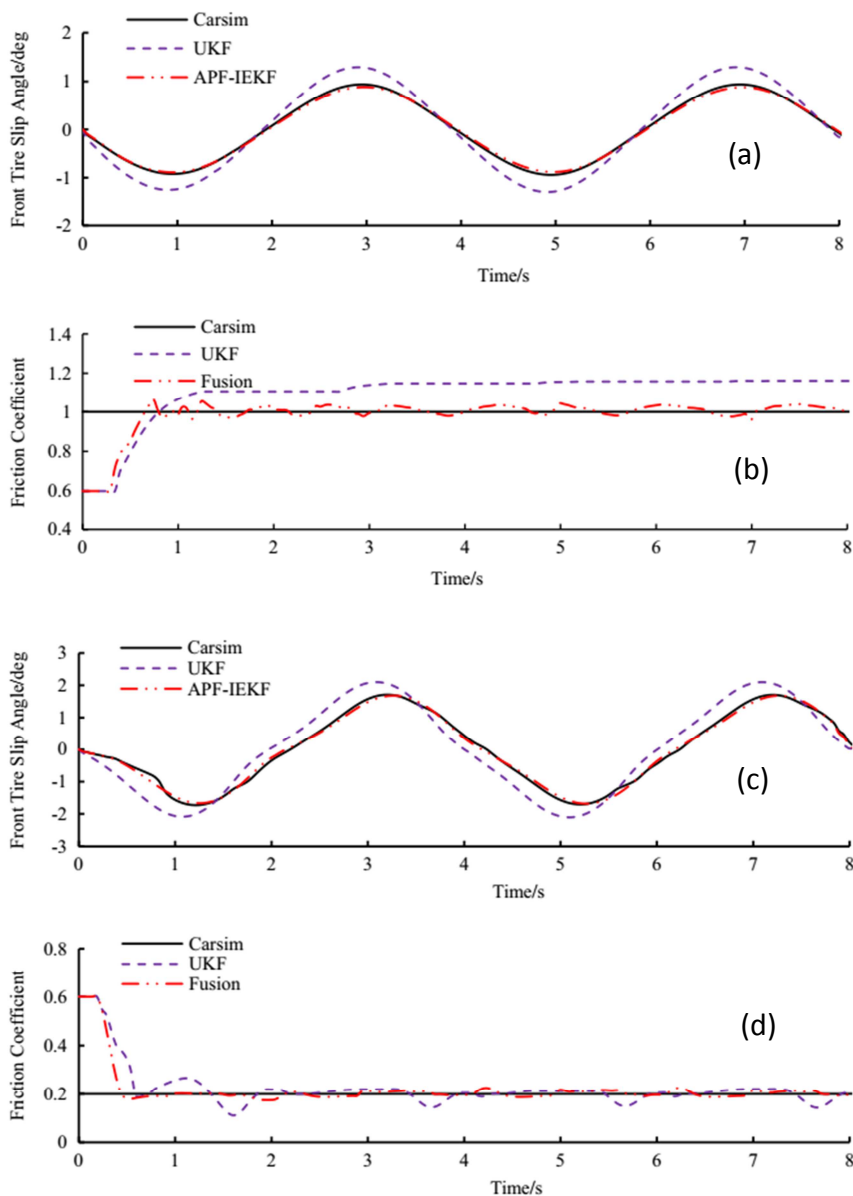


Fig. 6 Tire-road friction curve using by Carsim, Unscented Kalman Filter (UKF), Combined Auxiliary Particle Filter and Iteration Extended Kalman Filter (APF-IEKF), and Fusion model, (a) and (b) estimation under high friction coefficient, (c) and (d) estimation under low friction coefficient [39]

3.5 ROAD PROFILE ESTIMATION

Road profiles such as road geometries, deformations, and irregularities persistently modify the wheel orientations as well as vehicle positions. Therefore, road profile estimation is one of the most crucial parameters to estimate vehicle performance. Accordingly, road profile knowledge is inevitable for road roughness index evaluation, road quality estimation, suspension system design, vehicle dynamics analysis and control [62,63]. For road profile estimation tools, analysing vehicle data are paramount [64]. The road profile estimation technique can be divided into two classifications; direct and indirect road profile estimations based on vehicle responses. These estimation methods have been widely discussed. However, the direct profile estimation

techniques such as the full car (FC) model [65], artificial neural network (ANN) approach [66], Particle Filter and a Half Car (HC) model [67,68], 1-DOF model [69], the road profile estimation algorithms using Kalman Filters [70], and Youla-Kučera parametric observer [62] have been utilized. These techniques firstly determine the road profile estimation and then transform it into the road indices [71]. These indices can approximate road profiles reasonably for vehicles, though there may require proper calibration with drive tests.

Researchers have also extensively studied such as power spectrum density (PSD) [72] and the quarter car (QC) model [73]. The profile estimation problem can be solved in a stochastic framework using the QC model. Xue et al. [71] discussed these direct and indirect road profile estimation techniques with their usability and limitations and they estimated the road profile using the augmented Kalman filter (AKF) and Rauch-Tung-Striebel (RTS) smoothing model as shown in Figure 7 (profile distance: 9 km, sampling interval: 0.05 m, driving speed: 60 km/h).

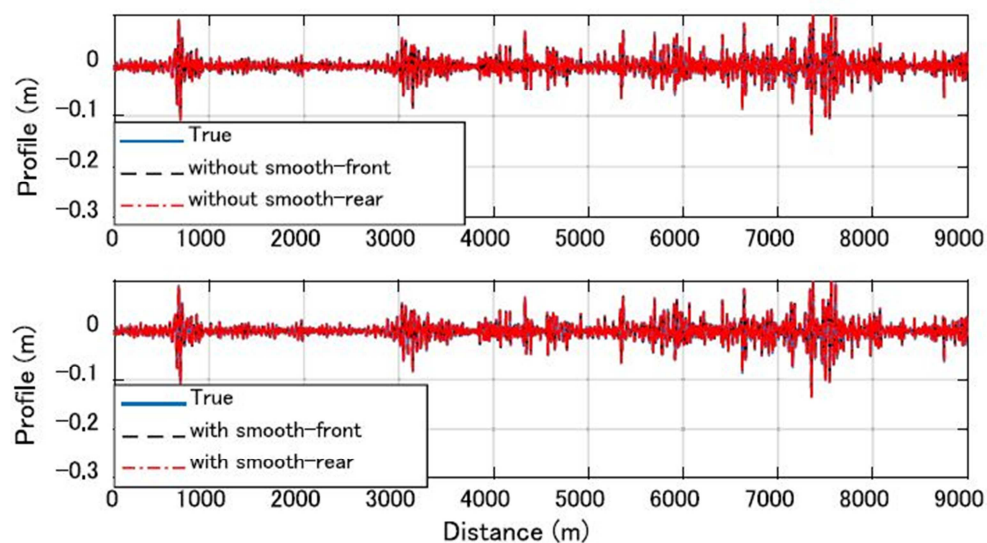


Fig. 7 Road profile estimation using augmented Kalman filter (AKF) and Rauch-Tung-Striebel (RTS) smoothing model [71]

3.6 ROLL ANGLE ESTIMATION

The roll angle estimation is directly related to the lateral forces and is known as the 'absolute roll angle' that can be measured with respect to gravity. Poor roll stability is one of the main reasons for the high rate of fatal vehicle crashes and acute damage as they become prone to changing their rollover. Thus, the roll stability of a vehicle is a crucial parameter for vehicle dynamics. Researchers have focused on developing the Electronic Stability Control (ESC) system, Global Positioning System (GPS), Roll Stability Control (RSC) system, and Inertial Navigation System (INS) to actuate the vehicle rolling system parameters [25,74,75]. For designing an RSC system, it needs to fulfil some requirements such as fast response time of actuators, real-time, high data sampling frequency, integration of all elements, and cost [74]. Roll angle can be estimated using various types of sensors: accelerometer and angular rate sensors [76], inertial angle sensor and gyroscope [77], lateral tire force sensors [78], vehicle dashboard sensors [79], roll rate and yaw rate sensors [80]. These various sensors use the technique of Kalman Filter [78], artificial intelligence approach [25,81], and robust estimator's techniques [80].

3.7 ADVANCED TECHNOLOGIES FOR VEHICLE STATE ESTIMATION

The methods for increasing computational efficiency, reduction of power consumption in electric devices, high stability in vehicle dynamics along with a high variety of networking protocols and information and communication technologies (ICTs) are being used in the manoeuvre vehicle dynamic controls [64]. Researchers have developed many smart modules for vehicle state estimation like the NN module, Kalman Module, inertial navigation system (INS), virtual longitudinal force estimation sensors (VLF), and global positioning system (GPS) [74,82,83]. In [84], vehicular ad hoc networks (VANETs) and three-valued, secure routing (VSR) are used for intelligent transport systems and vehicle control management. The study in the direct yaw control system (DYC) [85-87], active front steering system (AFS) [77,88], four-wheel steering system [89], collision avoidance system (CAS) [90], adaptive cruise control (ACC) [91] and acceleration slip regulation (ASR) have shown that the longitudinal drive stability and dynamic performance have been improved [92]. It is interesting to note that the different lateral acceleration and response were generated by changes in the steering wheel angle when the vehicle turns at a constant longitudinal speed. The vehicle response, such as the roll and yaw angle, may be measured to determine the transient behaviour of further suspension tuning activities [9]. Majid et al. [93] also showed that the Semi Active Lateral Control (SALC) algorithm can be minimized roll overshoot differences among various lateral acceleration inputs for improved handling performance. It is worth noting that an anti-lock braking system (ABS) has improved human safety [94]. The chasm model has been used for developing the automotive control system and laser module [95] that are used in vehicle stability control systems and can maintain vehicle stability and passengers' safety even in extreme situations. However, these control systems need accurate information about vehicle sideslip angle, lateral and longitudinal forces in potential vehicle trajectories, and real-time road conditions for better vehicle dynamic management. In addition, these advanced systems need real-time knowledge and data of vehicle states for practical effects and effective performance [96]. However, some vehicle state estimations are complex to measure due to technical difficulties in complicated driving environments and the requirement of the high cost of vehicle sensors [97].

4. MODEL-BASED ANALYSIS

From the literature review, it is found that most researchers have discussed their research outcome related to some vital factors such as tire estimation, tire-road friction coefficient, lateral force, vertical force, side-slip angle, slip ratio, slip/toe angle, camber angle, roll angle, lateral torque, rolling /friction force, tire inflation pressure, tire load, tire wear, energy consumption, vehicle speed, suspension parameters, steering parameters, road conditions, and weather condition, etc. These factors have been analysed with both experimental and model-based method where in most cases model-based analysis supported the experimental results.

Therefore, according to continuation in research, our experimental method is developed based on the concept of [20] and [95] which both focused on the regression model and wheel alignment inspection process. It has been found that the regression model has maintained a good correlation between the dependent variable and independent variable with our experimental data.

4.1 EXPERIMENTAL SETUP AND DATA ANALYSIS

The experiment has been performed using a wheel alignment machine (Best-5800) on TOYOTA ECHO PLUS-2ZZ-GE-02 light vehicle, as shown in Figure 8.

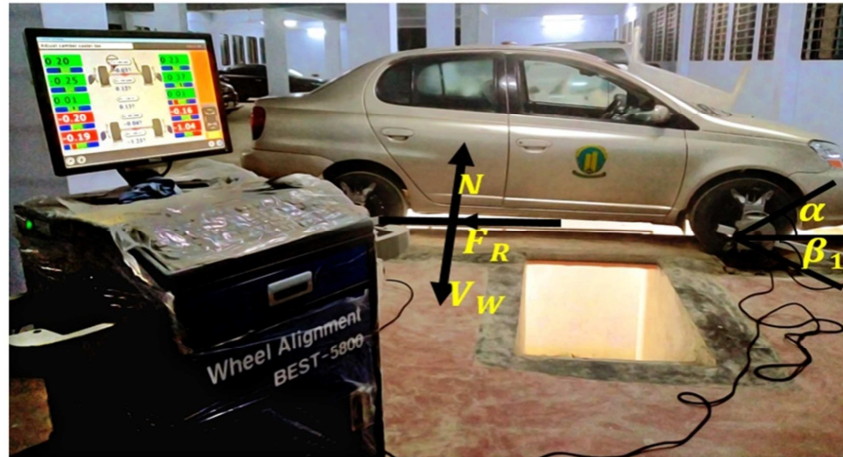


Fig. 8 The experimental setup using a wheel alignment machine (Best-5800)

During the test performance following testing environment and related parameters are maintained:

Experimental test conditions:

Weather temperature = (17.56°C to 31.23°C), humidity = (30.00% to 72.67%), engine outer temperature = (78.37°C to 82.70°C) and number of test run, $n = 20$.

Vehicle particulars:

Vehicle Model: TOYOTA ECHO PLUS-2ZZ-GE-02

Engine displacement: 1300 cc

Tire Size: 175/70R14

Vehicle weight: 965 kg

Air condition system: Non air condition

Gear position: Auto transmission

Type of fuel: Octane

Alignment conditions:

Caster angle (Left) = 0.20°

Caster angle (Right) = 0.23°

Camber angle (Left) = -0.25°

Camber angle (Right) = -0.37°

Tire pressure (Front and Rear) = 32 psi

Speed = 30 km/h,

Travelling distance = 6 km

Driver and one passenger weight = 125 kg

Suspension conditions:

LH FRONT Suspension Weight: 1.49 kN

Adherence: 57%,

RH FRONT Suspension Weight: 1.76 kN

Adherence: 60%,

LH REAR Suspension Weight: 1.1 kN

Adherence: 45%,

RH REAR Suspension Weight: 1.12 kN

Adherence: 51%

Engine cylinder performance conditions:

Cylinder-1 = 80.63%

Cylinder-2 = 80.10%

Cylinder-3 = 80.63%

Cylinder-4 = 80.10%

Table 2 shows the experimental data for various misalignment values of Front Right Slip/toe-in angles and corresponding fuel consumption increment with respect to fuel consumption at no-misalignment conditions.

Table 2 Experimental data for 20 test runs

Front Right Slip/Toe-in Angle, α (deg.)	Rolling Resistance Coefficient, $\mu_{RRC} = \frac{F_R}{V_W}$ (dimensionless)	Rolling Resistance Force, $F_R = (\mu_{RRC} \times V_W)$ (N)	Energy Consumption, $E_c = (F_R \times T_d)$ (KJ)	Fuel Consumption, F_c (ml)	% of fuel consumption increment w.r.t. no-misalignment condition
0.00	0.0210	224.4223	1346.5340	348	0.00
0.08	0.0210	224.5165	1347.0993	353	1.44
0.20	0.0210	224.8698	1349.2189	356	2.30
0.35	0.0211	225.9440	1355.6639	361	3.74
0.50	0.0214	228.4441	1370.6648	368	5.75
0.65	0.0216	231.4860	1388.9161	374	7.47
0.80	0.0221	236.7870	1420.7217	382	9.77
0.95	0.0227	242.5483	1455.2900	389	11.78
1.10	0.0233	249.3131	1495.8788	396	13.79
1.25	0.0241	258.2162	1549.2972	404	16.09
1.40	0.0251	268.3038	1609.8228	412	18.39
1.55	0.0260	278.0466	1668.2794	419	20.40
1.70	0.0271	290.1626	1740.9755	427	22.70
1.84	0.0282	301.5662	1809.3974	434	24.71
2.00	0.0295	315.4460	1892.6760	442	27.01
2.14	0.0307	328.2719	1969.6313	449	29.02
2.25	0.0321	343.6346	2061.8078	457	31.32
2.36	0.0334	357.6301	2145.7804	464	33.33
2.43	0.0346	369.9908	2219.9450	470	35.06
2.53	0.0364	389.0772	2334.4632	479	37.64

4.2 DATA ANALYSIS AND CORRELATION DEVELOPMENT

From Figure 9, it is seen that the changes in front right slip/toe-in angle (from 0.00° to 2.53°) cause the effect of changes in rolling resistance coefficient from 0.0210 to 0.0364, the rolling resistance force from 224.42 N to 389.077 N, energy consumption from 1346.53 KJ to 2334.46 KJ and fuel consumption from 348 ml to 479 ml for the car. The test results found that the maximum increment of fuel consumption due to misalignment reaches 37.64%. Therefore, it is proved that if rolling resistance/friction increases due to misalignment, the fuel consumption also increases.

Based on the experimental results, the strength of correlation between front right toe-in angle and fuel consumption is found using Pearson’s correlation coefficient, as shown in Eq. (11).

$$r_{xy} = \frac{\sum_{i=1}^n (x_i - \bar{x})(y_j - \bar{y})}{\sqrt{\sum_{i=1}^n (x_i - \bar{x})^2 \sum_{i=1}^n (y_j - \bar{y})^2}} \quad (11)$$

Where:

$$x_i = \alpha_i = 0.00^\circ$$

$$y_j = f_c = 348 \text{ ml}$$

$$\bar{x} = \bar{\alpha} = 1.30^\circ$$

$$\bar{y} = \bar{f} = 408.85 \text{ ml}$$

$$r_{xy} = r_{\alpha f_c} = 0.99$$

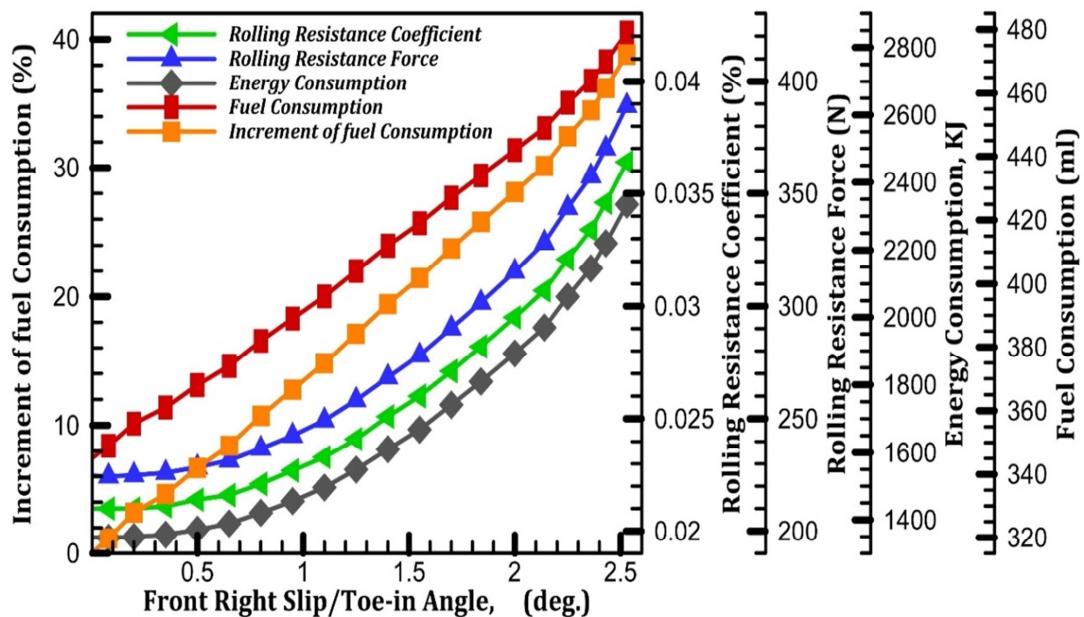


Fig. 9 Variation of rolling resistance coefficient, Rolling resistance Force, Energy consumption, increment of fuel consumption with respect to Front right slip/toe-in angle

The correlation coefficient (r_{xy}) is found 0.99 which is within the range of $1 > r_{xy} > 0.75$. It proves that there is a very strong positive correlation between the front right toe-in angle and fuel consumption of the light vehicle.

After that, four correlation models are developed using the regression method. These are:

- i) Model 1: Correlation between the front right toe-in angle and fuel consumption;
- ii) Model 2: Correlation between rolling resistance coefficient and fuel consumption;
- iii) Model 3: Correlation between rolling resistance force and fuel consumption;
- iv) Model 4: Correlation between energy consumption and fuel consumption.

The R square and adjusted R square values of the corresponding regression model are shown in Table 3, and P-values in Table 4. The regression models are found, as below:

$$\text{Fuel Consumption} = 343.57 + 50.327 \times \text{Front right toe-in angle for Model 1}$$

$$\text{Fuel Consumption} = 198.17 + 8079.27 \times \text{Rolling resistance coefficient for Model 2}$$

Fuel Consumption = 197.99 + 0.76 × Rolling resistance force for Model 3

Fuel Consumption = 197.99 + 0.126 × Energy consumption for Model 4

Table 3 The R square, adjusted R square values and P-value

Regression Model no.	Multiple R	R Square	Adjusted R Square	Standard Error	Observations
1	0.997051614	0.99411192	0.993784804	3.329811883	20
2	0.972924071	0.946581247	0.943613539	10.02951008	20
3	0.973146606	0.947014316	0.944070667	9.988772473	20
4	0.973146568	0.947014243	0.944070589	9.988779385	20

Table 4 P-values for the regression models

Regression Model no.		Coefficients	Standard Error	t Stat	P-value
1	Intercept	343.5736217	1.404120757	244.6895112	3.71138E-33
	Front Right Toe-in Angle	50.3269772	0.912922275	55.1273406	1.58195E-21
2	Intercept	198.1694539	12.02711919	16.47688451	2.65196E-12
	Rolling Resistance Coefficient	8079.270526	452.3804421	17.85946025	6.73321E-13
3	Intercept	197.9941925	11.98522381	16.51985775	2.5375E-12
	Rolling Resistance Force	0.755834713	0.042139714	17.93639881	6.25628E-13
4	Intercept	197.9941768	11.98523342	16.5198432	2.53753E-12
	Energy Consumption	0.125972458	0.007023291	17.9363857	6.25636E-13

In model 1, R^2 value is found 0.99411192. It can be said that 99.41% of the variation in the fuel consumption rate is explained by the front right toe-in angle. Also, the $R^2 = 0.9941$ and adjusted $R^2 = 0.9937$ are very close and the p-values are less than 0.05, therefore, it can be claimed that it is a true relationship between front right toe-in angle and fuel consumption.

Similarly, model-2, model-3, and model-4 also show a true relationship between the dependent and independent variables. This indicates that the correlation R-square = 99.41%, 94.65%, 94.70%, and 94.70% tend toward 1, so the variance of the fuel consumption can be explained by the regression model. Thus, an acceptable regression model can be used to explain the relation of factors determining the fuel consumption rate.

5. CONCLUSION

In this paper, a comprehensive review work has been presented for relevant vehicle dynamic states estimation with vehicle stability control applications. Most recent research articles have been reviewed from different aspects of estimation approaches. The estimation techniques discussed in this article will be helpful for future researchers in respect of vehicle dynamic states. Various estimation models based techniques are extensively used to estimate the vehicle dynamic states based on dynamics and observers have been studied and their pros and cons have also been discussed. Apart from the model-based techniques and non-model-based approaches such as ANN, fuzzy logic has also been discussed. The effectiveness of these models may vary with driving conditions, passengers, and seating arrangements. However, any appropriate and exact model-based technique is not proven yet in the production of vehicle industries. Thus, the most appropriate technique is needed to coordinate from model-based estimation techniques, which could vastly be improving the performance of the vehicle stability and control. In this research, four regression models have been developed based on experimental data after verifying with Pearson's correlation coefficient.

Much more research is needed in vehicle dynamics fields like (a) dynamic model considering linearity and non-linearity in the vehicle system, (b) tire friction and tire surface, and (c) the quality and reliability of the sensors, actuators, and microprocessor, which are crucial for the advanced or intelligent control system.

Finally, a summary has been presented in the upcoming advanced automotive technology related to the vehicle dynamic state estimation and control stability. These modern technologies are presently not fully matured for vehicle control stability. So, significant researches on vehicle dynamics and control stability have to be conducted with much more qualitative outcomes.

6. ACKNOWLEDGMENTS

The author would like to acknowledge the Research and Funding section of Chittagong University of Engineering and Technology for their financial support to continue the project. The author would also like to thank the Faculty members of the Department of Mechanical Engineering for their support and for providing lab facilities.

7. CONFLICTS OF INTEREST

The authors declare that there is no conflict of interests regarding the publication of this paper.

NOMENCLATURE

x	= Values of the front right toe-in angle (deg.)	MBS	= Multi Body system
\bar{x}	= Mean of the values of the front right toe-in angle (deg.)	FEM	= Finite Element Method
f_c	= Values of the fuel consumption (ml)	BEM	= Boundary Element Method
\bar{f}	= Mean of the values of the fuel	ABS	= Anti-lock Braking System
		ACC	= Adaptive Cruise Control

$r_{\alpha fc}$	= consumption (ml) Pearson's correlation coefficient (dimensionless) for front right toe-in angle and fuel consumption.	ESC	= Electronic Stability Control
V_s	= Vehicle speed (m/s)	ACC	= Active Chassis Control
μ_{RRC}	= Rolling resistance coefficient (dimensionless)	EKF	= Extended Kalman Filter
F_R	= Rolling resistance Force (N)	GPS	= Global Positioning System
V_W	= Vehicle weight (N)	APF	= Auxiliary Particle Filter
T_d	= Travelling distance (m)	IEKF	= Iteration Extended Kalman Filter
T_p	= Tire pressure (psi)	FCM	= Full Car Model
E_c	= Energy consumption (KJ)	ANN	= Artificial Neural Network
df	= Degrees of freedom	HCM	= Half Car Model
SS	= Sum of Square	DoF	= Degree of Freedom
MS	= Mean Squared error	PSD	= Power Spectrum Density
α	= Front right toe-in angle (deg.)	QCM	= Quarter Car Model
β_1	= Front right toe-out angle (deg.)	AKF	= Augmented Kalman Filter
y	= Lateral displacement (m)	RTS	= Rauch Tung Striebel
ψ	= Yaw angle (deg.)	RSC	= Roll Stability Control
ω	= Rotational velocity (rev/s)	INS	= Inertial Navigation System
V_x	= Longitudinal velocity (m/s)	ICTs	= Information and Communication Technologies
λ	= Tire slip ratio	VLF	= Virtual Longitudinal Force
θ	= Roll angle (deg.)	VANETs	= Vehicular Ad hoc Networks
F	= Tire camber force (N)	VSR	= Valued Secure Routing
γ	= Camber angle (deg.)	DYC	= Direct Yaw Control
		AFS	= Active Front Steering
		CAS	= Collision Avoidance System
		ASR	= Acceleration Slip Regulation

8. REFERENCES

- [1] V. Díaz, M. Ramírez, B. Muñoz, A wheel model for the study of the wheel angle measurement in the periodic motor vehicle inspection, *International Journal of Vehicle Design*, Vol. 34, No. 3, pp. 297-308, 2004. <https://doi.org/10.1504/IJVD.2004.003963>
- [2] J-S. Young, H-Y. Hsu, C-Y. Chuang, Camber angle inspection for vehicle wheel alignments, *Sensors*, Vol. 17, No. 2, pp. 285, 2017. <https://doi.org/10.3390/s17020285>
- [3] K.B. Singh, M.A. Arat, S. Taheri, Literature review and fundamental approaches for vehicle and tire state estimation, *Vehicle System Dynamics*, Vol. 57, No. 11, pp. 1643-1665, 2018. <https://doi.org/10.1080/00423114.2018.1544373>
- [4] C. Cheng, D. Cebon, Parameter and state estimation for articulated heavy vehicles, *Vehicle System Dynamics*, Vol. 49, No. 1-2, pp. 399-418, 2011. <https://doi.org/10.1080/00423110903406656>

- [5] F. Du, Z. Guan, J. Li, Y. Cai, D. Wu, Dynamics Modeling of Active Full-Wheel Steering Vehicle Based on Simulink, *International Conference on Mechatronics and Intelligent Robotics*, Springer, Singapore, pp. 3-17, 2019.
https://doi.org/10.1007/978-981-15-0238-5_1
- [6] A. Chebly, R. Talj, A. Charara, Coupled longitudinal/lateral controllers for autonomous vehicles navigation, with experimental validation, *Control Engineering Practice*, Vol. 88, pp. 79-96, 2019. <https://doi.org/10.1016/j.conengprac.2019.05.001>
- [7] C.A. Vivas-Lopez, J.C. Tudon-Martinez, D. Hernandez-Alcantara, R. Morales-Menendez, Global chassis control system using uspension, steering, and braking subsystems, *Mathematical Problems in Engineering*, Vol. 2015, 2015.
<https://doi.org/10.1155/2015/263424>
- [8] Y. Chen, J.J. Zhu, Car-like ground vehicle trajectory tracking by using trajectory linearization control, *In Dynamic Systems and Control Conference*, Vol. 58288, pp. V002T21A014, American Society of Mechanical Engineers, 2017.
<https://doi.org/10.1115/DSCC2017-5372>
- [9] P. Lunger, J. Edelmann, Basics of Vehicle Dynamics, Vehicle Models, *In Vehicle Dynamics of Modern Passenger Cars*, pp. 1-45, Springer, Cham, 2019.
https://doi.org/10.1007/978-3-319-79008-4_1
- [10] R.N. Jazar, *Vehicle Dynamics: Theory and Application*, Springer, 2017.
https://doi.org/10.1007/978-3-319-53441-1_2
- [11] G. Rill, A.A. Castro, *Road Vehicle Dynamics: Fundamentals and Modeling with MATLAB®*, CRC Press, 2020. <https://doi.org/10.1201/9780429244476>
- [12] R. Ghandour, A. Victorino, A. Charara, D. Lechner, A vehicle skid indicator based on maximum friction estimation, *IFAC Proceedings*, Vol. 44, No. 1, pp. 2272-2277, 2011.
<https://doi.org/10.3182/20110828-6-IT-1002.02105>
- [13] W. Zhang, N. Ding, G. Yu, W. Zhou, Virtual sensors design in vehicle sideslip angle and velocity of the centre of gravity estimation, *In 2009 9th International Conference on Electronic Measurement & Instruments*, pp. 3-652, IEEE, 2009.
<https://doi.org/10.1109/ICEMI.2009.5274228>
- [14] H.F. Grip, L. Imsland, T.A. Johansen, J.C. Kalkkuhl, A. Suissa, Vehicle sideslip estimation, *IEEE Control Systems Magazine*, Vol. 29, No. 5, pp. 36-52, 2009.
<https://doi.org/10.1109/MCS.2009.934083>
- [15] H.K. Fathy, D. Kang, J.L. Stein, Online vehicle mass estimation using recursive least squares and supervisory data extraction, *In 2008 American Control Conference*, pp. 1842-1848, IEEE, 2008. <https://doi.org/10.1109/ACC.2008.4586760>
- [16] T. Hsiao, N-C. Liu, S-Y. Chen, Robust estimation of the friction forces generated by each tire of a vehicle, *In Proceedings of the 2011 American Control Conference*, pp. 5261-5266, IEEE, 2011.
- [17] Q. Cheng, A. Correa-Victorino, A. Charara, A new nonlinear observer using unscented Kalman filter to estimate sideslip angle, lateral tire road forces and tire road friction coefficient, *In 2011 IEEE Intelligent Vehicles Symposium (IV)*, pp. 709-714, IEEE, 2011.

<https://doi.org/10.1109/IVS.2011.5940501>

- [18] K. Nam, S. Oh, H. Fujimoto, Y. Hori, Vehicle state estimation for advanced vehicle motion control using novel lateral tire force sensors, *In Proceedings of the 2011 American Control Conference*, pp. 4853-4858, IEEE, 2011.
<https://doi.org/10.1109/ACC.2011.5990916>
- [19] D. Garcia-Pozuelo, J. Yunta, O. Olatunbosun, X. Yang, V. Diaz, A strain-based method to estimate slip angle and tire working conditions for intelligent tires using fuzzy logic, *Sensors*, Vol. 17, No. 4, pp. 874, 2017. <https://doi.org/10.3390/s17040874>
- [20] K.B. Singh, S. Taheri, Accelerometer based method for tire load and slip angle estimation, *Vibration*, Vol. 2, No. 2, pp. 174-186, 2019.
<https://doi.org/10.3390/vibration2020011>
- [21] S. Mavromatis, A. Laiou, G. Yannis, Safety assessment of control design parameters through vehicle dynamics model, *Accident Analysis & Prevention*, Vol. 125, pp. 330-335, 2019. <https://doi.org/10.1016/j.aap.2018.07.016>
- [22] A. Rehm, Estimation of vehicle roll angle, *In 2010 4th International Symposium on Communications, Control and Signal Processing (ISCCSP)*, pp. 1-4, IEEE, 2010.
<https://doi.org/10.1109/ISCCSP.2010.5463458>
- [23] L. Hu, W. Yang, J. He, H. Zhou, Z. Zhang, X. Luo, R. Zhao, L. Tang, P. Du, Roll angle estimation using low cost MEMS sensors for paddy field machine, *Computers and Electronics in Agriculture*, Vol. 158, pp. 183-188, 2019.
<https://doi.org/10.1016/j.compag.2019.01.010>
- [24] H.B. Jeong, S.H. You, H.H. Kang, C.K. Ahn, Vehicle roll angle and bank angle estimation using FIR filtering, *In 2017 Eighth International Conference on Intelligent Control and Information Processing (ICICIP)*, pp. 348-352, IEEE, 2017.
<https://doi.org/10.1109/ICICIP.2017.8113969>
- [25] L. Vargas Meléndez, B.L. Boada, M.J.L. Boada, A. Gauchía, V. Díaz, A sensor fusion method based on an integrated neural network and Kalman filter for vehicle roll angle estimation, *Sensors*, Vol. 16, No. 9, pp. 1400, 2016. <https://doi.org/10.3390/s16091400>
- [26] M. Tanelli, S. Savaresi, C. Cantoni, Longitudinal vehicle speed estimation for traction and braking control systems, *In 2006 IEEE International Symposium on Intelligent Control*, pp. 2790-2795, IEEE, 2006. <https://doi.org/10.1109/CCA.2006.286032>
- [27] M.L.H. Abd Rahman, K. Hudha, Z. Abd Kadir, N.H. Amer, M. Murrad, Simulation Study on the Vehicle Speed Control in Longitudinal Direction using a New Continuously Variable Transmission (CVT) System, *Journal of Mechanical Engineering*, Vol SI 7 (1), pp. 127-146, 2018.
- [28] X. Chen, N. Xu, K. Guo, Tire wear estimation based on nonlinear lateral dynamic of multi-axle steering vehicle, *International Journal of Automotive Technology*, Vol. 19, No. 1, pp. 63-75, 2018. <https://doi.org/10.1007/s12239-018-0007-2>
- [29] B. Samadi, R. Kazemi, K.Y. Nikravesh, M. Kabganian, Real-time estimation of vehicle state and tire-road friction forces, *In Proceedings of the 2001 American Control Conference (Cat. No. 01CH37148)*, Vol. 5, pp. 3318-3323, IEEE, 2001.
<https://doi.org/10.1109/ACC.2001.946140>

- [30] Y. Sebsadji, S. Glaser, S. Mammar, J. Dakhlallah, Road slope and vehicle dynamics estimation, *In 2008 American Control Conference*, pp. 4603-4608, IEEE, 2008.
<https://doi.org/10.1109/ACC.2008.4587221>
- [31] J. Dakhlallah, S. Glaser, S. Mammar, Y. Sebsadji, Tire-road forces estimation using extended Kalman filter and sideslip angle evaluation, *In 2008 American Control Conference*, pp. 4597-4602, IEEE, 2008.
<https://doi.org/10.1109/ACC.2008.4587220>
- [32] R.N. Jazar, A. Subic, N. Zhang, Kinematics of a smart variable caster mechanism for a vehicle steerable wheel, *Vehicle System Dynamics*, Vol. 50, No. 12, pp. 1861-1875, 2012.
<https://doi.org/10.1080/00423114.2012.699075>
- [33] A. Pattathil, S. Kumar, S. Iqbal, 1D Tire Model Parameter Synthesis for Vehicle Handling Targets Assessment - A Strategy of Optimization and Evaluation of Tire Math's, No. 2019-26-0361, *SAE Technical Paper*, 2019. <https://doi.org/10.4271/2019-26-0361>
- [34] S. Cheng, L. Li, B. Yan, C. Liu, X. Wang, J. Fang, Simultaneous estimation of tire side-slip angle and lateral tire force for vehicle lateral stability control, *Mechanical Systems and Signal Processing*, Vol. 132, pp. 168-182, 2019.
<https://doi.org/10.1016/j.ymssp.2019.06.022>
- [35] C. Ludwig, C.S. Kim, Influence of testing surface on tire lateral force characteristics-Einfluss der Prüfoberfläche auf die Reifenseitenkraft-Eigenschaften, *In 8th International Munich Chassis Symposium 2017*, pp. 795-808. Springer Vieweg, Wiesbaden, 2017.
https://doi.org/10.1007/978-3-658-18459-9_54
- [36] E. Lee, J. Lee, S.B. Choi, String tyre model for evaluating steering agility performance using tyre cornering force and lateral static characteristics, *Vehicle System Dynamics*, Vol. 55, No. 2, pp. 231-243, 2017. <https://doi.org/10.1080/00423114.2016.1252048>
- [37] W. Cho, J. Yoon, S. Yim, B. Koo, K. Yi, Estimation of tire forces for application to vehicle stability control, *IEEE Transactions on Vehicular Technology*, Vol. 59, No. 2, pp. 638-649, 2009. <https://doi.org/10.1109/TVT.2009.2034268>
- [38] Y. Tian, Y. Lian, C. Tian, Z. Sun, K. Liu, Sideslip Angle and Tire Cornering Stiffness Estimations for Four-In-Wheel-Motor-Driven Electric Vehicles, *In 2019 Chinese Control Conference (CCC)*, pp. 2418-2423, IEEE, 2019.
<https://doi.org/10.23919/ChiCC.2019.8866066>
- [39] Y-H. Liu, T. Li, Y-Y. Yang, X-W. Ji, J. Wu, Estimation of tire-road friction coefficient based on combined APF-IEKF and iteration algorithm, *Mechanical Systems and Signal Processing*, Vol. 88, pp. 25-35, 2017. <https://doi.org/10.1016/j.ymssp.2016.07.024>
- [40] M. Doumiati, A. Victorino, A. Charara, D. Lechner, Unscented Kalman filter for real-time vehicle lateral tire forces and sideslip angle estimation, *In 2009 IEEE Intelligent Vehicles Symposium*, pp. 901-906, IEEE, 2009.
- [41] W. Botes, T.R. Botha, P. Schalk Els, Sideslip Angle Estimation Using a Kinematics Based Unscented Kalman Filter and Digital Image Correlation, *In The IAVSD International Symposium on Dynamics of Vehicles on Roads and Tracks*, pp. 1635-1642, Springer, Cham, 2019. https://doi.org/10.1007/978-3-030-38077-9_186
- [42] K.B. Singh, Virtual sensor for real-time estimation of the vehicle sideslip angle, *Sensor Review*, Vol. 40 No. 2, pp. 255-272, 2020. <https://doi.org/10.1108/SR-11-2018-0300>

- [43] E.A. Wan, R. Van Der Merwe, The unscented Kalman filter for nonlinear estimation, *In Proceedings of the IEEE 2000 Adaptive Systems for Signal Processing, Communications, and Control Symposium* (Cat. No. 00EX373), pp. 153-158, IEEE, 2000.
- [44] L.A. McGee, S.F. Schmidt, Discovery of the Kalman filter as a practical tool for aerospace and industry, NASA Technical Memorandum; 86847, 1985.
- [45] L. Tong, An approach for vehicle state estimation using extended Kalman filter, *In International Computer Science Conference*, pp. 56-63, Springer, Berlin, Heidelberg, 2012. https://doi.org/10.1007/978-3-642-34381-0_7
- [46] M. Doumiati, A. Correa-Victorino, A. Charara, D. Lechner, On board real-time estimation of vehicle lateral tire-road forces and sideslip angle, *IEEE/ASME Transactions on Mechatronics*, Vol. 16, No. 4, pp. 601-614, 2010. <https://doi.org/10.1109/TMECH.2010.2048118>
- [47] J.K. Uhlmann, Dynamic map building and localization: New theoretical foundations, PhD diss., University of Oxford- 1995.
- [48] D.Q. Vo, H. Marzbani, M. Fard, R.N. Jazar, Caster-Camber Relationship in Vehicles, *In Nonlinear Approaches in Engineering Applications*, pp. 63-89, Springer, Cham, 2016. https://doi.org/10.1007/978-3-319-27055-5_2
- [49] H-B. Huang, Y-J. Chiu, X-X. Jin, Numerical calculation of irregular tire wear caused by tread self-excited vibration and sensitivity analysis, *Journal of Mechanical Science and Technology*, Vol. 27, No. 7, pp. 1923-1931, 2013. <https://doi.org/10.1007/s12206-013-0505-0>
- [50] M. Klüppel, Wear and abrasion of tires, *Encyclopedia of Polymeric Nanomaterials*, Vol. 2015, pp. 2600-2604, 2015. https://doi.org/10.1007/978-3-642-29648-2_312
- [51] J. Yang, G.L. Wang, Z.J. Wan, C. Liang, H.C. Zhou, Non-natural equilibrium contour design for radial tire and its influence on tire performance, *International Journal of Automotive Technology*, Vol. 17, No. 4, pp. 639-649, 2016. <https://doi.org/10.1007/s12239-016-0063-4>
- [52] S.G. Zuo, T.X. Ni, X.D. Wu, K. Wu, X.W. Yang, Prediction procedure for wear distribution of transient rolling tire, *International Journal of Automotive Technology*, Vol. 15, No. 3, pp. 505-515, 2014. <https://doi.org/10.1007/s12239-014-0053-3>
- [53] L. Rodríguez-Tembleque, R. Abascal, M.H. Aliabadi, A boundary elements formulation for 3D fretting-wear problems, *Engineering Analysis with Boundary Elements*, Vol. 35, No. 7, pp. 935-943, 2011. <https://doi.org/10.1016/j.enganabound.2011.03.002>
- [54] S. Knisley, A correlation between rolling tire contact friction energy and indoor tread wear, *Tire Science and Technology*, Vol. 30, No. 2, pp. 83-99, 2002. <https://doi.org/10.2346/1.2135251>
- [55] L. Ma, J. Wang, L. Xu, M. Ouyang, Optimized Torque Distribution Strategy for In-Wheel-Drive Electric Vehicles to Reduce Tire Wear, *In 2015 IEEE Vehicle Power and Propulsion Conference (VPPC)*, pp. 1-5, IEEE, 2015. <https://doi.org/10.1109/VPPC.2015.7352991>

- [56] Y.H. Shen, Y. Gao, T. Xu, Multi-axle vehicle dynamics stability control algorithm with all independent drive wheel, *International Journal of Automotive Technology*, Vol. 17, No. 5, pp. 795-805, 2016. <https://doi.org/10.1007/s12239-016-0078-x>
- [57] S. Khaleghian, A. Emami, S. Taheri, A technical survey on tire-road friction estimation, *Friction*, Vol. 5, No. 2, pp. 123-146, 2001). <https://doi.org/10.1007/s40544-017-0151-0>
- [58] M. Schinkel, K. Hunt, Anti-lock braking control using a sliding mode like approach, *In Proceedings of the 2002 American Control Conference* (IEEE Cat. No. CH37301), Vol. 3, pp. 2386-2391, IEEE, 2002. <https://doi.org/10.1109/ACC.2002.1023999>
- [59] L-Q. Jin, M. Ling, W. Yue, Tire-road friction estimation and traction control strategy for motorized electric vehicle, *PLoS ONE*, Vol. 12, No. 6, pp. e0179526, 2017. <https://doi.org/10.1371/journal.pone.0179526>
- [60] M. Yu, B. Xiao, Z. You, G. Wu, X. Li, Y. Ding, Dynamic friction coefficient between tire and compacted asphalt mixtures using tire-pavement dynamic friction analyzer, *Construction and Building Materials*, Vol. 258, pp. 119492, 2020. <https://doi.org/10.1016/j.conbuildmat.2020.119492>
- [61] L. Li, K. Yang, G. Jia, X. Ran, J. Song, Z-Q. Han, Comprehensive tire-road friction coefficient estimation based on signal fusion method under complex maneuvering operations, *Mechanical Systems and Signal Processing*, Vol. 56, pp. 259-276, 2015. <https://doi.org/10.1016/j.ymsp.2014.10.006>
- [62] M. Doumiati, J. Martinez, O. Sename, L. Dugard, D. Lechner, Road profile estimation using an adaptive Youla-Kučera parametric observer: Comparison to real profilers, *Control Engineering Practice*, Vol. 61, pp. 270-278, 2017. <https://doi.org/10.1016/j.conengprac.2015.12.020>
- [63] S.A. Abu Bakar, M.M. Abdul Majid, S. Mansor, M.K. Abdul Hamid, Z.C. Daud, Performance Comparison Between Skyhook and Semi Active Damping Force Estimator (SADE) Algorithms for Semi Active Suspension System, *Journal of Mechanical Engineering*, Vol SI 6 (1), 143-159, 2018.
- [64] N. Jin, T.S. Paraskeva, E.G. Dimitrakopoulos, Estimation of bridge frequencies from a passing vehicle, *Maintenance, Safety, Risk, Management and Life-Cycle Performance of Bridges, Proceedings of the 9th International Conference on Bridge Maintenance, Safety and Management*, pp. 2566-2572, 2018. <https://doi.org/10.1201/9781315189390-347>
- [65] H. Imine, Y. Delanne, N.K. M'sirdi, Road profile inputs for evaluation of the loads on the wheels, *Vehicle System Dynamics*, Vol. 43, No. sup1, pp. 359-369, 2005. <https://doi.org/10.1080/00423110500108945>
- [66] A. Solhmirzaei, S. Azadi, R. Kazemi, Road profile estimation using wavelet neural network and 7-DOF vehicle dynamic systems, *Journal of Mechanical Science and Technology*, Vol. 26, No. 10, pp. 3029-3036, 2012. <https://doi.org/10.1007/s12206-012-0812-x>
- [67] H. Wang, T. Nagayama, J. Nakasuka, B. Zhao, D. Su, Extraction of bridge fundamental frequency from estimated vehicle excitation through a particle filter approach, *Journal of Sound and Vibration*, Vol. 428, pp. 44-58, 2018.

<https://doi.org/10.1016/j.jsv.2018.04.030>

- [68] H. Wang, T. Nagayama, B. Zhao, D. Su, Identification of moving vehicle parameters using bridge responses and estimated bridge pavement roughness, *Engineering Structures*, Vol. 153, pp. 57-70, 2017. <https://doi.org/10.1016/j.engstruct.2017.10.006>
- [69] K. Yagi, A measuring method of road surface longitudinal profile from sprung acceleration, and verification with road profiler, *Journal of Japan Society of Civil Engineers*, Ser. E1 (Pavement Engineering), Vol. 69, No. 3, 2013. https://doi.org/10.2208/jscejpe.69.1_1
- [70] S-W. Kang, J-S. Kim, G-W. Kim, Road roughness estimation based on discrete Kalman filter with unknown input, *Vehicle System Dynamics*, Vol. 57, No. 10, pp.1530-1544, 2019.
- [71] K. Xue, T. Nagayama, B. Zhao, Road profile estimation and half-car model identification through the automated processing of smartphone data, *Mechanical Systems and Signal Processing*, Vol. 142, pp. 106722, 2020. <https://doi.org/10.1016/j.ymsp.2020.106722>
- [72] A. González, E.J. O'brien, Y-Y. Li, K. Cashell, The use of vehicle acceleration measurements to estimate road roughness, *Vehicle System Dynamics*, Vol. 46, No. 6, pp. 483-499, 2008. <https://doi.org/10.1080/00423110701485050>
- [73] T. Nagayama, A. Miyajima, S. Kimura, Y. Shimada, Y. Fujino, Road condition evaluation using the vibration response of ordinary vehicles and synchronously recorded movies, *In Sensors and Smart Structures Technologies for Civil, Mechanical, and Aerospace Systems 2013*, Vol. 8692, pp. 86923A, International Society for Optics and Photonics, 2013. <https://doi.org/10.1117/12.2010074>
- [74] J. García Guzmán, L. Prieto González, J. Pajares Redondo, M.M. Montalvo Martinez, M.J.L. Boada, Real-time vehicle roll angle estimation based on neural networks in IoT low-cost devices, *Sensors*, Vol. 18, No. 7, pp. 2188, 2018. <https://doi.org/10.3390/s18072188>
- [75] J. Ryu E.J. Rossetter, J.C. Gerdes, Vehicle sideslip and roll parameter estimation using GPS, *In Proceedings of the AVEC International Symposium on Advanced Vehicle Control*, pp. 373-380, 2002.
- [76] R. Tafner, M. Reichhartinger, M. Horn, Robust online roll dynamics identification of a vehicle using sliding mode concepts, *Control Engineering Practice*, Vol. 29, pp. 235-246, 2014. <https://doi.org/10.1016/j.conengprac.2014.03.002>
- [77] R. Rajamani, D. Piyabongkarn, V. Tsourapas, J.Y. Lew, Real-time estimation of roll angle and CG height for active rollover prevention applications, *In 2009 American Control Conference*, pp. 433-438, IEEE, 2009. <https://doi.org/10.1109/ACC.2009.5160045>
- [78] K. Nam, S. Oh, H. Fujimoto, Y. Hori, Estimation of sideslip and roll angles of electric vehicles using lateral tire force sensors through RLS and Kalman filter approaches, *IEEE Transactions on Industrial Electronics*, Vol. 60, No. 3, pp. 988-1000, 2012. <https://doi.org/10.1109/TIE.2012.2188874>
- [79] G. Jiang, L. Liu, C. Guo, J. Chen, F. Muhammad, X. Miao, A novel fusion algorithm for estimation of the side-slip angle and the roll angle of a vehicle with optimized key parameters, *Proceedings of the Institution of Mechanical Engineers, Part D: Journal of Automobile Engineering*, Vol. 231, No. 2, pp. 161-174, 2017. <https://doi.org/10.1177/0954407016644879>

- [80] B.L. Boada, M.J.L. Boada, V. Diaz, A robust observer based on energy-to-peak filtering in combination with neural networks for parameter varying systems and its application to vehicle roll angle estimation, *Mechatronics*, Vol. 50, pp. 196-204, 2018.
<https://doi.org/10.1016/j.mechatronics.2018.02.008>
- [81] M.J.L. Boada, B.L. Boada, A.G. Babe, J.A.C. Ramos, V.D. Lopez, Active roll control using reinforcement learning for a single unit heavy vehicle, *International Journal of Heavy Vehicle Systems*, Vol. 16, No. 4, pp. 412-430, 2009.
<https://doi.org/10.1504/IJHVS.2009.027413>
- [82] K.B. Singh, Vehicle sideslip angle estimation based on tire model adaptation, *Electronics*, Vol. 8, No. 2, pp. 199, 2019. <https://doi.org/10.3390/electronics8020199>
- [83] Q. Xia, L. Chen, X. Xu, Y. Cai, H. Jiang, T. Chen, G. Pan, Running States Estimation of Autonomous Four-Wheel Independent Drive Electric Vehicle by Virtual Longitudinal Force Sensors, *Mathematical Problems in Engineering*, Vol. 2019, 2019.
<https://doi.org/10.1155/2019/8302943>
- [84] M. Sohail, L. Wang, 3VSR: three valued secure routing for vehicular ad hoc networks using sensing logic in adversarial environment, *Sensors*, Vol. 18, No. 3, pp. 856, 2018.
<https://doi.org/10.3390/s18030856>
- [85] A. Goodarzi, E. Esmailzadeh, Design of a VDC system for all-wheel independent drive vehicles, *IEEE/ASME Transactions on Mechatronics*, Vol. 12, No. 6, pp. 632-639, 2007.
<https://doi.org/10.1109/TMECH.2007.910075>
- [86] H. Zhang, X. Zhang, J. Wang, Robust gain-scheduling energy-to-peak control of vehicle lateral dynamics stabilization, *Vehicle System Dynamics*, Vol. 52, No. 3, pp. 309-340, 2014. <https://doi.org/10.1080/00423114.2013.879190>
- [87] X. Jin, Z. Yu, G. Yin, J. Wang, Improving vehicle handling stability based on combined AFS and DYC system via robust Takagi-Sugeno fuzzy control, *IEEE Transactions on Intelligent Transportation Systems*, Vol. 19, No. 8, pp. 2696-2707, 2017.
<https://doi.org/10.1109/TITS.2017.2754140>
- [88] X. Jin, G. Yin, C. Bian, J. Chen, P. Li, N. Chen, Gain-scheduled vehicle handling stability control via integration of active front steering and suspension systems, *Journal of Dynamic Systems, Measurement, and Control*, Vol. 138, No. 1, 2016.
<https://doi.org/10.1115/1.4031629>
- [89] Q. Tan, L. Shi, J. Katupitiya, A novel control approach for path tracking of a force-controlled two-wheel-steer four-wheel-drive vehicle, *Proceedings of the Institution of Mechanical Engineers, Part D: Journal of Automobile Engineering*, Vol. 233, No. 6, pp.1480-1494, 2019. <https://doi.org/10.1177/0954407018760433>
- [90] Y. Lian, Y. Zhao, L. Hu, Y. Tian, Longitudinal collision avoidance control of electric vehicles based on a new safety distance model and constrained-regenerative-braking-strength-continuity braking force distribution strategy, *IEEE Transactions on Vehicular Technology*, Vol. 65, No. 6, pp.4079-4094, 2015.
<https://doi.org/10.1109/TVT.2015.2498949>

- [91] A. Weißman, D. Görge, X. Lin, Energy-optimal adaptive cruise control combining model predictive control and dynamic programming, *Control Engineering Practice*, Vol. 72, pp. 125-137, 2018. <https://doi.org/10.1016/j.conengprac.2017.12.001>
- [92] H. He, J. Peng, R. Xiong, H. Fan, An acceleration slip regulation strategy for four-wheel drive electric vehicles based on sliding mode control, *Energies*, Vol. 7, No. 6, pp. 3748-3763, 2014. <https://doi.org/10.3390/en7063748>
- [93] M.M. Abdul Majid, M.S. Salleh, M.A. Abu Hashim, N.H. Ismail, S. Mansor, S.A. Abu Bakar, Performance of Semi Active Lateral Control (SALC) Algorithm for Semi Active Suspension System in Multibody Co-Simulation Method, *Journal of Mechanical Engineering*, Vol. SI 6 (1), pp. 5-65, 2018.
- [94] S.Lj. Perić, D.S. Antić, M.B. Milovanović, D.B. Mitić, M.T. Milojković, S.S. Nikolić, Quasi-sliding mode control with orthogonal endocrine neural network-based estimator applied in anti-lock braking system, *IEEE/ASME Transactions on Mechatronics*, Vol. 21, No. 2, pp. 754-764, 2015. <https://doi.org/10.1109/TMECH.2015.2492682>
- [95] S.H. Kim, K.I. Lee, Wheel Alignment of a Suspension Module Unit Using a Laser Module, *Sensors*, Vol. 20, No. 6, pp. 1648, 2020. <https://doi.org/10.3390/s20061648>
- [96] X. Jin, G. Yin, N. Chen, Advanced estimation techniques for vehicle system dynamic state: A survey, *Sensors*, Vol. 19, No. 19, pp. 4289, 2019. <https://doi.org/10.3390/s19194289>
- [97] D. Piyabongkarn, R. Rajamani, J.A. Grogg, J.Y. Lew, Development and experimental evaluation of a slip angle estimator for vehicle stability control, *IEEE Transactions on Control Systems Technology*, Vol. 17, No. 1, pp. 78-88, 2008. <https://doi.org/10.1109/TCST.2008.922503>